EUROPEAN ORGANIZATION FOR NUCLEAR RESEARCH

L3 Note 2514
March 7, 2000

Preliminary Results on the Measurement of W-Pair Cross Sections in e^+e^- Interactions at $\sqrt{s} = 192 - 202$ GeV and W-Decay Branching Fractions

The L3 Collaboration

Abstract

We report on the measurement of W-boson pair-production with the L3 detector at LEP. In a data sample corresponding to a total luminosity of 233.3 pb^{-1} collected at centre-of-mass energies of 192, 196, 200 and 202 GeV, we select 3529 four-fermion events with pairs of hadronic jets or pairs of leptons with high invariant masses. Branching fractions of W decays into different fermion-antifermion pairs are determined. Assuming charged-current lepton universality, the branching fraction for hadronic W decays is measured to be: $B(\mathrm{W} \to \mathrm{hadrons}) = 68.47 \pm 0.49\ (stat.) \pm 0.33\ (syst.)$ %, including data collected at lower centre-of-mass energies. Combining all final states the total cross section for W-pair production is measured at the four centre-of-mass energies. These results are preliminary.

Submitted to *2000 Winter Conferences*

1 Introduction

For the 1999 data taking period, the centre-of-mass energy, $\sqrt{s}$, of the e^+e^- collider LEP at CERN was increased in several steps to 192, 196, 200 and finally 202 GeV. These energies are well above the kinematic threshold of W-boson pair production, $e^+e^- \to W^+W^-$.

To lowest order within the Standard Model [1], three Feynman diagrams contribute to W-pair production, the s-channel γ and Z-boson exchange and the t-channel ν_e exchange, referred to as CC03 [2–4]. The W boson decays into a quark-antiquark pair, for example $W^- \to \bar{u}d$ or $\bar{c}s$, or a lepton-antilepton pair, $W^- \to \ell^- \bar{\nu}_\ell$ ($\ell = e, \mu, \tau$); in the following denoted as qq, $\ell\nu$ or ff in general for both W^+ and W^- decays. In this letter, measurements of all four-fermion final states mediated by W-pair production are reported:

1. $e^+e^- \to \ell\nu\ell\nu(\gamma)$ 2. $e^+e^- \to qqe\nu(\gamma)$ 3. $e^+e^- \to qq\mu\nu(\gamma)$

4. $e^+e^- \to qq\tau\nu(\gamma)$ 5. $e^+e^- \to qqqq(\gamma)$,

where (γ) indicates the possible presence of radiative photons. Additional contributions to the production of four-fermion final states arising from other neutral-current (NC) or charged-current (CC) Feynman diagrams are small. At the current level of statistical accuracy the interference effects need to be taken into account only for $e^+e^- \to \ell\nu\ell\nu(\gamma)$ (CC56+NC56) and $e^+e^- \to qqe\nu(\gamma)$ (CC20) [2–4].

During the 1999 run the L3 detector collected an integrated luminosity of 29.7 pb^{-1} at $\sqrt{s} = 191.60$ (hereafter called 192) GeV, 83.7 pb^{-1} at $\sqrt{s} = 195.54$ (196) GeV, 82.8 pb^{-1} at $\sqrt{s} = 199.54$ (200) GeV, and 37.0 pb^{-1} at $\sqrt{s} = 201.75$ (200) GeV. These centre-of-mass energies are known to ± 0.04 GeV [5].

The cross section is measured for all four-fermion final states mediated by W-pair production. Combining these preliminary measurements W-decay branching fractions and the total W-pair production cross section are determined with significantly improved precision compared to earlier measurements with less luminosity reported by L3 [6–9] and other LEP experiments [10]. The large amount of luminosity collected in 1999 enables a precise measurement of cross sections at $\sqrt{s} = 192 - 202$ GeV and a significant improvement in the determination of W-decay branching fractions.

2 Analysis of Four-Fermion Production

The L3 detector is described in detail in Reference 11. The selections of the four-fermion final states are similar to the ones used at $\sqrt{s}$ of 161 GeV [6], 172 GeV [7], 183 GeV [8], and 189 GeV [9]. Charged leptons are explicitly identified using their characteristic signature. In general, electrons are identified as energy depositions in the BGO electromagnetic calorimeter with electromagnetic shower shape which are matched in azimuth to a track reconstructed in the central tracking chamber (TEC). Muons are identified either as tracks reconstructed in the muon chambers pointing back to the interaction vertex or by their minimum-ionising-particle (MIP) signature. Jets arising from hadronic τ decays are reconstructed based on a jet-clustering inside a cone of 15° half-opening angle [12]. Hadronic jets corresponding to quarks are reconstructed using the Durham jet algorithm [13] and adding four-momenta during the combination process. The momentum of the neutrino in $e^+e^- \to qq\ell\nu$ events is identified with the missing momentum vector.

Selection efficiencies and background contaminations of all processes are determined by

Monte Carlo simulations. The following Monte Carlo event generators are used to simulate the various signal and background processes: KORALW [14] and HERWIG [15] ($e^+e^- \to WW \to ffff(\gamma)$); EXCALIBUR [16] ($e^+e^- \to ffff(\gamma)$); PYTHIA [17] ($e^+e^- \to q\bar{q}(\gamma), ZZ(\gamma)$); KORALZ [18] ($e^+e^- \to \mu^+\mu^-(\gamma)$, $\tau^+\tau^-(\gamma)$); BHAGENE3 [19], BHWIDE [20] and TEEGG [21] ($e^+e^- \to e^+e^-(\gamma)$), DIAG36 [22] and LEP4F [23] (leptonic two-photon collisions); PHOJET [24] (hadronic two-photon collisions). The response of the L3 detector is modelled with the GEANT [25] detector simulation program which includes the effects of energy loss, multiple scattering and showering in the detector material. Hadronic showers are simulated with the GHEISHA [26] program.

The measurement of the total luminosity, $\mathcal{L}$, follows the procedure described in Reference 27. The preliminary total error on the luminosity measurement for the 1999 data is estimated to be 0.65%.

The results on cross sections and W-decay branching fractions are determined in a combined analysis taking migration between the various final states into account [6–9]. The results are compared to the predictions of the Standard Model calculated for a mass of the W boson of $M_W = 80.33$ GeV [28] using the GENTLE [29] program.

2.1 $e^+e^- \to \ell\nu\ell\nu(\gamma)$

The event selection for the process $e^+e^- \to \ell\nu\ell\nu(\gamma)$ requires two charged leptons and missing energy due to the neutrinos. The selection depends on whether the event contains zero, one or two identified electrons or muons, referred to as jet-jet, lepton-jet and lepton-lepton class. Electrons, muons and τ jets are identified inside the polar angular range of $|\cos\theta| < 0.96$. For events with one or two electrons, one electron should lie in the angular range $|\cos\theta| < 0.92$ in order to limit the amount of background from Bhabha scattering. For events containing jets only, the two highest energy jets must also satisfy $|\cos\theta| < 0.92$.

A total of 283 events is selected in the data: 183 lepton-lepton events, 84 lepton-jet events and 16 jet-jet events. The distributions of the acoplanarity between the two charged leptons for lepton-lepton events, and of the lepton energy for lepton-jet events are shown in Figure 1.

The signal efficiencies are determined from CC56+NC56 Monte Carlo samples within the following phase-space cuts: $|\cos\theta| < 0.96$ for both charged leptons, with energies larger than 15 GeV and 5 GeV, respectively. Efficiencies are given in the form of a 6 by 6 matrix, as shown in Table 1, relating $\ell\nu\ell\nu$ events at four-fermion level to $\ell\nu\ell\nu$ events at reconstruction level. The background contributions are listed in Table 2. A total systematic error of 4.7% on the measured cross section is obtained.

2.2 $e^+e^- \to qqe\nu(\gamma)$

The event selection for the process $e^+e^- \to qqe\nu(\gamma)$ requires an identified electron of at least 20 GeV, high particle multiplicity arising from the $q\bar{q}$ system, and missing momentum due to the neutrino.

A total of 485 events is selected in the data: 476 events with the electron identified in the BGO electromagnetic calorimeter and nine events with the electron identified in the SPACAL calorimeter. The distributions of the polar angle of the neutrino, the energy of the electron, the electron-neutrino invariant mass and the invariant mass of the jet-jet system are shown in Figure 2.

The signal efficiency is determined from a CC20 Monte Carlo sample within the following

phase-space cuts: $E_{\mathrm{e}}, E_{\nu} > 20$ GeV; $|\cos\theta_{\mathrm{e}}|, |\cos\theta_{\nu}| < 0.95$; $M_{\mathrm{e}\nu}, M_{qq} > 45$ GeV. The selection efficiencies and the background contributions are listed in Tables 1 and 2. A total systematic error of 2.0% on the measured cross section is obtained.

2.3 $\mathrm{e^+e^-} \to qq\mu\nu(\gamma)$

The event selection for the process $\mathrm{e^+e^-} \to qq\mu\nu(\gamma)$ requires high particle multiplicity arising from the $q\bar{q}$ system, an identified muon and missing momentum due to the neutrino.

A total of 431 events is selected in the data: 401 events with a muon reconstructed in the muon spectrometer and 30 events with a muon identified by its MIP signature. The distributions of the angle between the muon and the nearest of the two reconstructed hadronic jets, the momentum of the muon, the muon-neutrino invariant mass and the invariant mass of the jet-jet system are shown in Figure 3. The selection efficiencies and background contribution are listed in Tables 1 and 2. A total systematic error of 3.0% on the measured cross section is obtained.

2.4 $\mathrm{e^+e^-} \to qq\tau\nu(\gamma)$

The event selection for the process $\mathrm{e^+e^-} \to qq\tau\nu(\gamma)$ is based on the identification of a tau jet in a hadronic event with missing energy.

A total of 469 events is selected in the data: 51 $\tau \to \nu\mathrm{e}\bar{\nu}$ events, 63 $\tau \to \nu\mu\bar{\nu}$ events and 355 $\tau \to \nu$hadrons events. The distributions of the number of TEC tracks associated to the τ jet and of the invariant mass of the $q\bar{q}$ system are shown in Figure 4. The selection efficiencies and the background contributions are listed in Tables 1 and 2. A total systematic error of 4.3% on the measured cross section is obtained.

2.5 $\mathrm{e^+e^-} \to qqqq(\gamma)$

The event selection for the process $\mathrm{e^+e^-} \to qqqq(\gamma)$ is based on a neural network applied to a sample of pre-selected events. The pre-selection accepts 94% of the WW $\to qqqq(\gamma)$ signal while reducing the dominating $\mathrm{e^+e^-} \to q\bar{q}(\gamma)$ background by a factor of 15. The network is trained such that the output peaks at one for the signal and at zero for the background. The distribution of the neural-network output is shown in Figure 6.

The neural-network output distribution for data events is fitted by a linear combination of neural-network output distributions derived from Monte Carlo simulations for signal and background [6–9]. The results of the fit for the signal cross sections are shown in Table 3, as well as in Table 5. The results for the $\mathrm{e^+e^-} \to q\bar{q}(\gamma)$ background cross sections at the four centre-of-mass energies are 101.4 ± 8.3 pb, 85.8 ± 4.8 pb, 93.5 ± 5.1 pb and 78.6 ± 7.2 pb respectively, where the errors are only statistical; these values are in good agreement with the Standard Model prediction.

As a cross check the signal cross section is determined by applying a cut on the output of the neural network larger than 0.6, which minimises the expected statistical error. The selection efficiencies (at $\sqrt{s} = 200$ GeV) and the background contributions corresponding to this cut are listed in Tables 1 and 2. A total of 1861 events is selected in the data, yielding signal cross sections at the four centre-of-mass energies of 7.21 ± 0.59 pb, 7.23 ± 0.35 pb, 8.44 ± 0.38 pb and 7.98 ± 0.57 pb respectively, in good agreement with the results of the fit to the neural-network output distribution. A total systematic error of 1.8% on the measured cross section is obtained.

3 Results

The cross sections, σ_i, of the signal processes i are determined simultaneously in one maximum-likelihood fit, taking cross feed between final states into account. The fitting procedure to determine cross sections of the signal processes, W-decay branching fractions and the total W-pair cross section is identical to the one used previously [6–9].

For the purely leptonic final states the fitting procedure determines six different cross sections corresponding to all possible combinations of flavours of the two final-state lepton pairs. Since the data statistics for the $\ell\nu\ell\nu(\gamma)$ final state is low, the sum of these six cross sections is quoted as the cross section for the process $\mathrm{e^+e^-} \to \ell\nu\ell\nu(\gamma)$.

The total likelihood is given by the product of Poissonian probabilities, $P(N_i, \mu_i)$, corresponding to the signal processes i having N_i selected events as listed in Table 2. The expected number of events for process i, μ_i, is calculated as:

$$\mu_i \;=\; \left(\sum_{j=1}^{10} \epsilon_{ij}\sigma_j + \sigma_i^{\mathrm{bg}} \right) \cdot \mathcal{L}\,, \tag{1}$$

where ϵ_{ij} is the efficiency of selection i to accept events from process j, σ_i^{bg} is the remaining background cross section arising from other processes. These numbers are listed in Tables 1 and 2. For the $\mathrm{e^+e^-} \to qqqq(\gamma)$ process, the Poissonian probability is replaced by the likelihood as a function of the signal cross section derived from the fit described in Section 2.5.

3.1 Signal Cross Sections

For the $qqe\nu(\gamma)$ and the six $\ell\nu\ell\nu(\gamma)$ final states the cross sections are determined within phase-space cuts to reduce contributions from processes not mediated by resonant W-pair production. In order to determine W-pair cross sections for these final states the measured cross sections are scaled by a multiplicative factor, f_i, as listed in Table 2. The conversion factors f_i are given by the ratio of the total CC03 cross section and the four-fermion cross section within phase-space cuts, and are calculated within the Standard Model using EXCALIBUR.

The resulting cross sections including statistical and systematic errors are listed in Table 3. The Standard Model agrees well with these results. Since the efficiency matrix of Table 1 contains non-zero off-diagonal elements, the five cross sections are correlated. The largest correlations, -11% and -19%, arise among the semileptonic channels between $qq\tau\nu$ and $qqe\nu$ and between $qq\tau\nu$ and $qq\mu\nu$. All other correlations are smaller than 1% in magnitude and thus negligible.

3.2 W-Decay Branching Fractions and W-Pair Cross Section

For the determination of the total CC03 production cross section of W-pairs, σ_{WW}, the signal cross sections σ_i are replaced by the product $r_i\sigma_{\mathrm{WW}}$ or $r_i\sigma_{\mathrm{WW}}/f_i$ for the $qqe\nu(\gamma)$ and $\ell\nu\ell\nu(\gamma)$ final states. The ratios r_i are given in terms of the W-decay branching fractions, $B(\mathrm{W} \to qq)$ and $B(\mathrm{W} \to \ell\nu)$, as follows: $r_{qqqq} = [B(\mathrm{W} \to qq)]^2$, $r_{qq\ell\nu} = 2B(\mathrm{W} \to qq)B(\mathrm{W} \to \ell\nu)$, and $r_{\ell\nu\ell\nu} = [B(\mathrm{W} \to \ell\nu)]^2$ for identical and $r_{\ell\nu\ell'\nu'} = 2B(\mathrm{W} \to \ell\nu)B(\mathrm{W} \to \ell'\nu')$ for different lepton flavours in the final state. The sum of the hadronic and the three leptonic branching fractions is constrained to be unity. For the determination of W-decay branching fractions the data collected at $\sqrt{s}$ of 161 GeV, 172 GeV, 183 GeV and 189 GeV are included.

The resulting W-decay branching fractions including statistical and systematic errors and correlations are listed in Table 4. The branching fractions are determined both with and without the assumption of charged-current lepton universality in W decays. The W-decay branching fractions obtained for the individual leptons are in good agreement with each other and support this assumption. Assuming lepton universality, the hadronic W-decay branching fraction is:

$$B(\mathrm{W} \to qq) \;=\; 68.47 \pm 0.49 \pm 0.33 \;\%\,, \tag{2}$$

where the first error is statistical and the second systematic. The accuracy on the W-decay branching fractions is significantly improved with respect to our previous publication based on the 1996, 1997 and 1998 data [6–9].

The branching fractions of the W boson depend on the six elements V_{ij} of the Cabibbo-Kobayashi-Maskawa quark mixing matrix V_{CKM} [30] not involving the top quark [3], $1/B(\mathrm{W} \to \ell\nu) = 3 + 3[1 + \alpha_{\mathrm{s}}(M_{\mathrm{W}})/\pi]V^2$, where α_{s} is the strong coupling constant. Our measurements correspond to:

$$V^2 \;=\; \sum_{i=\mathrm{u,c};\, j=\mathrm{d,s,b}} |V_{ij}|^2 \;=\; 2.091 \pm 0.047 \pm 0.032\,. \tag{3}$$

The sensitivity of this measurement to a single matrix element is largest for the dominant diagonal elements of V_{CKM}. Since V_{ud} is known much more precisely than V_{cs}, it is most useful to determine the latter. Using the current world-average values and errors of the other matrix elements not assuming the unitarity of V_{CKM} [31], the result is:

$$|V_{\mathrm{cs}}| \;=\; 1.021 \pm 0.023 \pm 0.015\,. \tag{4}$$

The statistical error includes the errors on α_{s} and the other V_{ij} but is dominated by the statistical error on the W branching fractions.

The W-pair cross sections are also derived imposing the W-decay branching fractions as expected within the Standard Model [3]. Results for the cross sections of the reactions $\mathrm{e^+e^-} \to \ell\nu\ell\nu(\gamma)$, $\mathrm{e^+e^-} \to qq\ell\nu(\gamma)$, $\mathrm{e^+e^-} \to qqqq(\gamma)$, and the total W-pair cross section, σ_{WW}, are shown in Table 5. The results for the total production cross section of W-pairs at the four centre-of-mass energies are:

$$\sqrt{s} = 191.60 \pm 0.04 \text{ GeV}: \qquad \sigma_{\mathrm{WW}} = 16.39 \pm 0.90 \pm 0.24 \text{ pb}\,, \tag{5}$$
$$\sqrt{s} = 195.54 \pm 0.04 \text{ GeV}: \qquad \sigma_{\mathrm{WW}} = 16.67 \pm 0.55 \pm 0.24 \text{ pb}\,, \tag{6}$$
$$\sqrt{s} = 199.54 \pm 0.04 \text{ GeV}: \qquad \sigma_{\mathrm{WW}} = 16.94 \pm 0.57 \pm 0.24 \text{ pb}\,, \tag{7}$$
$$\sqrt{s} = 201.75 \pm 0.04 \text{ GeV}: \qquad \sigma_{\mathrm{WW}} = 16.95 \pm 0.85 \pm 0.24 \text{ pb}\,. \tag{8}$$

Our published measurements of σ_{WW} at $\sqrt{s}$ of 161 GeV, 172 GeV, 183 GeV, our preliminary result at $\sqrt{s} = 189$ GeV, and the new preliminary results at $\sqrt{s} = 192 - 202$ GeV presented here are compared to the Standard Model expectation in Figure 7. The deviation from pure t-channel ν_{e} exchange in W-pair production is clearly visible. Both non-Abelian s-channel diagrams with triple-gauge-boson couplings as expected within the Standard Model are needed to obtain agreement with our measurements.

Recently, new preliminary predictions of the SM CC03 cross sections have appeared in the form of the Monte Carlo programs YFSWW3 [32] and RacoonWW [33]; both of these programs are still in a state of development. These preliminary predictions are respectively 2.0% and 2.4-2.8% lower than the ones from GENTLE and agree better with our data than GENTLE.

4 Acknowledgements

We wish to congratulate the CERN accelerator divisions for the successful upgrade of the LEP machine and to express our gratitude for its excellent performance. We acknowledge with appreciation the effort of the engineers, technicians and support staff who have participated in the construction and maintenance of this experiment.

References

[1] S. L. Glashow, Nucl. Phys. **22** (1961) 579;
S. Weinberg, Phys. Rev. Lett. **19** (1967) 1264;
A. Salam, in *Elementary Particle Theory*, ed. N. Svartholm, Stockholm, Almquist and Wiksell (1968), 367.

[2] D. Bardin *et al.*, Nucl. Phys. (Proc. Suppl.) **B 37** (1994) 148;
F.A. Berends *et al.*, Nucl. Phys. (Proc. Suppl.) **B 37** (1994) 163.

[3] W. Beenakker *et al.*, in *Physics at LEP 2*, Report CERN 96-01 (1996), eds G. Altarelli, T. Sjöstrand, F. Zwirner, Vol. 1, p. 79.

[4] D. Bardin *et al.*, in *Physics at LEP 2*, Report CERN 96-01 (1996), eds G. Altarelli, T. Sjöstrand, F. Zwirner, Vol. 2, p. 3.

[5] The LEP Energy Working Group, Private communication.

[6] The L3 Collaboration, M. Acciarri *et al.*, Phys. Lett. **B 398** (1997) 223.

[7] The L3 Collaboration, M. Acciarri *et al.*, Phys. Lett. **B 407** (1997) 419.

[8] The L3 Collaboration, M. Acciarri *et al.*, Phys. Lett. **B 436** (1998) 437.

[9] The W-Physics Analysis Group of the L3 Collaboration,
Preliminary Results on the Measurement of W-Pair Cross Sections in e^+e^- Interactions at $\sqrt{s}$ = 189 GeV and W-Decay Branching Fractions, L3 Note 2376, March 1999; paper #6_253 submitted to the International Europhysics Conference High Energy Physics 99, Tampere, Finland, 15-21 July 1999.

[10] The ALEPH Collaboration, R. Barate *et al.*, Phys. Lett. **B 401** (1997) 347, Phys. Lett. **B 415** (1997) 435, Phys. Lett. **B 453** (1999) 107;
The DELPHI Collaboration, P. Abreu *et al.*, Phys. Lett. **B 397** (1997) 158, Euro. Phys. Jour. **C 2** (1998) 581, Phys. Lett. **B 456** (1999) 310;
The OPAL Collaboration, K. Ackerstaff *et al.*, Phys. Lett. **B 389** (1996) 416, Euro. Phys. Jour. **C 1** (1998) 425, Euro. Phys. Jour. **C 8** (1999) 191.

[11] The L3 Collaboration, B. Adeva *et al.*, Nucl. Instr. and Meth. **A 289** (1990) 35;
M. Chemarin *et al.*, Nucl. Instr. and Meth. **A 349** (1994) 345;
M. Acciarri *et al.*, Nucl. Instr. and Meth. **A 351** (1994) 300;
G. Basti *et al.*, Nucl. Instr. and Meth. **A 374** (1996) 293;
I.C. Brock *et al.*, Nucl. Instr. and Meth. **A 381** (1996) 236;
A. Adam *et al.*, Nucl. Instr. and Meth. **A 383** (1996) 342.

[12] H.J. Daum *et al.*, Z. Phys. **C 8** (1981) 167.

[13] S. Catani *et al.*, Phys. Lett. **B 269** (1991) 432;
S. Bethke *et al.*, Nucl. Phys. **B 370** (1992) 310.

[14] KORALW version 1.33 is used.
M. Skrzypek, S. Jadach, W. Placzek and Z. Wąs, Comp. Phys. Comm. **94** (1996) 216;
M. Skrzypek, S. Jadach, M. Martinez, W. Placzek and Z. Wąs, Phys. Lett. **B 372** (1996) 289.

[15] HERWIG version 5.9 is used.
G. Marchesini and B. Webber, Nucl. Phys. **B 310** (1988) 461;
I.G. Knowles, Nucl. Phys. **B 310** (1988) 571;
G. Marchesini *et al.*, Comp. Phys. Comm. **67** (1992) 465.

[16] F.A. Berends, R. Kleiss and R. Pittau, Nucl. Phys. **B 424** (1994) 308; Nucl. Phys. **B 426** (1994) 344; Nucl. Phys. (Proc. Suppl.) **B 37** (1994) 163;
R. Kleiss and R. Pittau, Comp. Phys. Comm. **83** (1994) 141;
R. Pittau, Phys. Lett. **B 335** (1994) 490.

[17] PYTHIA version 5.722 is used.
T. Sjöstrand, *PYTHIA 5.7 and JETSET 7.4 Physics and Manual*,
CERN-TH/7112/93 (1993), revised August 1995; Comp. Phys. Comm. **82** (1994) 74.

[18] KORALZ version 4.02 is used.
S. Jadach, B. F. L. Ward and Z. Wąs, Comp. Phys. Comm. **79** (1994) 503.

[19] J.H. Field, Phys. Lett. **B 323** (1994) 432;
J.H. Field and T. Riemann, Comp. Phys. Comm. **94** (1996) 53.

[20] BHWIDE version 1.01 is used.
S. Jadach, W. Placzek, B.F.L. Ward, Phys. Rev. **D 40** (1989) 3582, Comp. Phys. Comm. **70** (1992) 305, Phys. Lett. **B 390** (1997) 298.

[21] D. Karlen, Nucl. Phys. **B 289** (1987) 23.

[22] F. A. Berends, P. H. Daverfeldt and R. Kleiss, Nucl. Phys. **B 253** (1985) 441.

[23] J.A.M. Vermaseren, J. Smith and G. Grammer Jr, Phys. Rev. **D 19** (1979) 137;
J.A.M. Vermaseren, Nucl. Phys. **B 229** (1983) 347.

[24] PHOJET version 1.05 is used.
R. Engel, Z. Phys. **C 66** (1995) 203; R. Engel and J. Ranft, Phys. Rev. **D 54** (1996) 4244.

[25] The L3 detector simulation is based on GEANT Version 3.15.
R. Brun *et al.*, *GEANT 3*, CERN-DD/EE/84-1 (Revised), 1987.
The GHEISHA program (H. Fesefeldt, RWTH Aachen Report PITHA 85/02 (1985))
is used to simulate hadronic interactions.

[26] H. Fesefeldt, RWTH Aachen Preprint PITHA 85/02 (1985).

[27] The L3 Collaboration, I.C. Brock *et al.*, Nucl. Instr. and Meth. **A 381** (1996) 236.

[28] The UA1 Collaboration, C. Albajar *et al.*, Z. Phys. **C 44** (1989) 15;
The UA2 Collaboration, J. Alitti *et al.*, Phys. Lett. **B 241** (1990) 150; Phys. Lett. **B 276** (1992) 354;
The CDF Collaboration, F. Abe *et al.*, Phys. Rev. Lett. **65** (1990) 2243; Phys. Rev. **D 43** (1991) 2070; Phys. Rev. Lett. **75** (1995) 11; Phys. Rev. **D 52** (1995) 4784;
The DØ Collaboration, S. Abachi *et al.*, Phys. Rev. Lett. **77** (1996) 3309.
We use the average value and error for the mass of the W boson as listed in:
R.M. Barnett *et al.*, *Review of Particle Properties*, Phys. Rev. **D 54** (1996) 1.

[29] GENTLE version 2.0 is used. D. Bardin *et al.*, Comp. Phys. Comm. **104** (1997) 161.

[30] N. Cabibbo, Phys. Rev. Lett. **10** (1963) 531;
M. Kobayashi and T. Maskawa, Prog. Theor. Phys. **49** (1973) 652.

[31] C. Caso *et al.*, *The 1998 Review of Particle Physics*, Euro. Phys. Jour. **C 3** (1998) 1.

[32] S. Jadach *et al.*, Phys. Lett. **B 417** (1998) 326; CERN-TH-99-222, UTHEP-98-0502, to be published in Phys. Rev. D.

[33] A. Denner *et al.*, BI-TP 99/45 (1999), *hep-ph/9912261.*

Selection of Process	Efficiencies [%] for									
	$e\nu e\nu$	$e\nu\mu\nu$	$e\nu\tau\nu$	$\mu\nu\mu\nu$	$\mu\nu\tau\nu$	$\tau\nu\tau\nu$	$qqe\nu$	$qq\mu\nu$	$qq\tau\nu$	$qqqq$
$e^+e^- \to e\nu e\nu(\gamma)$	63.7	0.3	12.8			1.1				
$e^+e^- \to e\nu\mu\nu(\gamma)$		58.3	9.6	0.6	10.9	1.6				
$e^+e^- \to e\nu\tau\nu(\gamma)$	5.3	1.2	34.6		0.1	6.6				
$e^+e^- \to \mu\nu\mu\nu(\gamma)$				50.0	8.4	0.8				
$e^+e^- \to \mu\nu\tau\nu(\gamma)$		2.6	0.2	2.2	28.8	4.0				
$e^+e^- \to \tau\nu\tau\nu(\gamma)$	0.1	0.1	1.9		0.9	18.9				
$e^+e^- \to qqe\nu(\gamma)$							86.1	0.2	2.2	
$e^+e^- \to qq\mu\nu(\gamma)$							0.1	71.2	4.8	
$e^+e^- \to qq\tau\nu(\gamma)$							5.0	6.7	48.1	0.3
$e^+e^- \to qqqq(\gamma)$							0.1		0.5	83.0

Table 1: Selection efficiencies for signal processes $e^+e^- \to \ell\nu\ell\nu(\gamma)$, $e^+e^- \to qq\ell\nu(\gamma)$, and $e^+e^- \to qqqq(\gamma)$, at $\sqrt{s} = 200$ GeV. For the $\ell\nu\ell\nu$ ($qqe\nu$) selections, the signal efficiency is derived from a CC56+NC56 (CC20) Monte Carlo sample and is given within phase-space cuts, see Section 2.1 (2.2). For the $qqqq$ selection, the numbers are quoted for a neural-network output larger than 0.60. Selection efficiencies at other centre-of-mass energies are only marginally different.

Selection of Process	192 GeV		196 GeV		200 GeV		202 GeV		
	N_{data}	Bg [pb]	N_{data}	Bg [pb]	N_{data}	Bg [pb]	N_{data}	Bg [pb]	f_i
$\mathrm{e^+e^-} \to \mathrm{e}\nu\mathrm{e}\nu(\gamma)$	9	0.136	28	0.138	15	0.146	8	0.146	0.87
$\mathrm{e^+e^-} \to \mathrm{e}\nu\mu\nu(\gamma)$	7	0.029	29	0.033	25	0.035	9	0.035	1.08
$\mathrm{e^+e^-} \to \mathrm{e}\nu\tau\nu(\gamma)$	5	0.011	17	0.015	20	0.030	10	0.030	1.08
$\mathrm{e^+e^-} \to \mu\nu\mu\nu(\gamma)$	7	0.087	17	0.085	19	0.056	10	0.056	0.96
$\mathrm{e^+e^-} \to \mu\nu\tau\nu(\gamma)$	5	0.006	11	0.007	13	0.008	3	0.008	1.12
$\mathrm{e^+e^-} \to \tau\nu\tau\nu(\gamma)$	2	0.020	7	0.018	6	0.011	1	0.011	0.96
$\mathrm{e^+e^-} \to qq\mathrm{e}\nu(\gamma)$	76	0.129	179	0.140	157	0.130	73	0.101	1.09
$\mathrm{e^+e^-} \to qq\mu\nu(\gamma)$	59	0.060	148	0.059	146	0.057	78	0.057	—
$\mathrm{e^+e^-} \to qq\tau\nu(\gamma)$	55	0.340	194	0.295	156	0.282	64	0.244	—
$\mathrm{e^+e^-} \to qqqq(\gamma)$	229	1.476	635	1.427	699	1.421	298	1.454	—

Table 2: Number of selected data events, N_{data}, and accepted background cross sections (Bg) from non-W processes for the selections of the signal processes $\mathrm{e^+e^-} \to \ell\nu\ell\nu(\gamma)$, $\mathrm{e^+e^-} \to qq\ell\nu(\gamma)$, and $\mathrm{e^+e^-} \to qqqq(\gamma)$, at the four different centre-of-mass energies. For the $qqqq$ selection, the numbers are quoted for a neural-network output larger than 0.60. The ratio of the CC03 cross section without cuts and the four-fermion cross section within phase-space cuts, f_i, is calculated with EXCALIBUR at $\sqrt{s} = 200$ GeV and listed in the last column; the dependence of these numbers on $\sqrt{s}$ is very small.

Process	N_{data}	N_{bg}	σ(CC03) [pb]	σ_{GENTLE} [pb]
$\sqrt{s} = 192$ GeV				
$\mathrm{e^+e^-} \to \ell\nu\ell\nu(\gamma)$	35	8.6	$1.51 \pm 0.35 \pm 0.07$	1.80 ± 0.04
$\mathrm{e^+e^-} \to qq\mathrm{e}\nu(\gamma)$	76	3.8	$2.93 \pm 0.36 \pm 0.06$	2.47 ± 0.05
$\mathrm{e^+e^-} \to qq\mu\nu(\gamma)$	59	1.8	$2.41 \pm 0.35 \pm 0.07$	2.47 ± 0.05
$\mathrm{e^+e^-} \to qq\tau\nu(\gamma)$	55	10.1	$2.19 \pm 0.48 \pm 0.10$	2.47 ± 0.05
$\mathrm{e^+e^-} \to qqqq(\gamma)$	229	43.9	$7.13 \pm 0.58 \pm 0.14$	7.73 ± 0.15
$\sqrt{s} = 196$ GeV				
$\mathrm{e^+e^-} \to \ell\nu\ell\nu(\gamma)$	109	24.2	$1.75 \pm 0.22 \pm 0.08$	1.83 ± 0.04
$\mathrm{e^+e^-} \to qq\mathrm{e}\nu(\gamma)$	179	11.7	$2.37 \pm 0.20 \pm 0.05$	2.52 ± 0.05
$\mathrm{e^+e^-} \to qq\mu\nu(\gamma)$	148	5.0	$2.08 \pm 0.20 \pm 0.06$	2.52 ± 0.05
$\mathrm{e^+e^-} \to qq\tau\nu(\gamma)$	194	24.7	$3.38 \pm 0.33 \pm 0.15$	2.52 ± 0.05
$\mathrm{e^+e^-} \to qqqq(\gamma)$	635	119.4	$7.41 \pm 0.36 \pm 0.14$	7.87 ± 0.16
$\sqrt{s} = 200$ GeV				
$\mathrm{e^+e^-} \to \ell\nu\ell\nu(\gamma)$	98	23.1	$1.66 \pm 0.22 \pm 0.08$	1.85 ± 0.04
$\mathrm{e^+e^-} \to qq\mathrm{e}\nu(\gamma)$	157	10.8	$2.14 \pm 0.19 \pm 0.04$	2.55 ± 0.05
$\mathrm{e^+e^-} \to qq\mu\nu(\gamma)$	146	4.7	$2.21 \pm 0.21 \pm 0.07$	2.55 ± 0.05
$\mathrm{e^+e^-} \to qq\tau\nu(\gamma)$	156	23.3	$2.75 \pm 0.32 \pm 0.12$	2.55 ± 0.05
$\mathrm{e^+e^-} \to qqqq(\gamma)$	699	117.7	$8.31 \pm 0.39 \pm 0.16$	7.96 ± 0.16
$\sqrt{s} = 202$ GeV				
$\mathrm{e^+e^-} \to \ell\nu\ell\nu(\gamma)$	41	10.6	$1.52 \pm 0.32 \pm 0.07$	1.86 ± 0.04
$\mathrm{e^+e^-} \to qq\mathrm{e}\nu(\gamma)$	73	3.7	$2.27 \pm 0.29 \pm 0.05$	2.56 ± 0.05
$\mathrm{e^+e^-} \to qq\mu\nu(\gamma)$	78	2.1	$2.66 \pm 0.33 \pm 0.08$	2.56 ± 0.05
$\mathrm{e^+e^-} \to qq\tau\nu(\gamma)$	64	9.0	$2.43 \pm 0.46 \pm 0.11$	2.56 ± 0.05
$\mathrm{e^+e^-} \to qqqq(\gamma)$	298	53.9	$7.98 \pm 0.57 \pm 0.15$	7.99 ± 0.16

Table 3: Number of selected data events, N_{data}, number of expected non-W background events, N_{bg}, and CC03 cross sections for the reactions $\mathrm{e^+e^-} \to qq\mathrm{e}\nu(\gamma)$, $\mathrm{e^+e^-} \to qq\mu\nu(\gamma)$, $\mathrm{e^+e^-} \to qq\tau\nu(\gamma)$, $\mathrm{e^+e^-} \to \ell\nu\ell\nu(\gamma)$ and $\mathrm{e^+e^-} \to qqqq(\gamma)$ at the four different centre-of-mass energies. For the $qqqq$ signal, the numbers N_{data} and N_{bg} correspond to a cut on the output of the neural network at 0.60, while the $qqqq$ cross section is obtained from a fit to the neural-network output distribution as described in Section 2.5. The first error is statistical and the second systematic. Also shown are the SM CC03 cross sections, σ_{GENTLE}, as calculated with GENTLE [29]. The theoretical error on the GENTLE cross sections amounts to 2% [3, 4].

Parameter	Lepton Non-Universality	Lepton Universality	Standard Model
$B(\mathrm{W} \to \mathrm{e}\nu)$ [%]	$10.22 \pm 0.33 \pm 0.14$	—	
$B(\mathrm{W} \to \mu\nu)$ [%]	$9.87 \pm 0.35 \pm 0.15$	—	
$B(\mathrm{W} \to \tau\nu)$ [%]	$11.64 \pm 0.47 \pm 0.21$	—	
$B(\mathrm{W} \to \ell\nu)$ [%]	—	$10.51 \pm 0.16 \pm 0.11$	10.83
$B(\mathrm{W} \to qq)$ [%]	$68.27 \pm 0.49 \pm 0.33$	$68.47 \pm 0.49 \pm 0.33$	67.51

Table 4: W-decay branching fractions, B, derived with and without the assumption of charged-current lepton universality. The correlations between the leptonic branching fractions are -0.026, -0.293, -0.337 for (eμ), (eτ), ($\mu\tau$), respectively. Also shown are the W-decay branching fractions [3] as expected in the Standard Model.

$\sqrt{s}$ [GeV]	$\sigma_{\ell\nu\ell\nu}$ [pb]	$\sigma_{qq\ell\nu}$ [pb]	σ_{qqqq} [pb]	σ_{WW} [pb]
191.60	$1.51 \pm 0.35 \pm 0.07$	$7.68 \pm 0.61 \pm 0.13$	$7.13 \pm 0.58 \pm 0.14$	$16.39 \pm 0.90 \pm 0.24$
195.54	$1.75 \pm 0.22 \pm 0.08$	$7.50 \pm 0.36 \pm 0.12$	$7.41 \pm 0.36 \pm 0.14$	$16.67 \pm 0.55 \pm 0.24$
199.54	$1.66 \pm 0.22 \pm 0.08$	$6.92 \pm 0.36 \pm 0.11$	$8.31 \pm 0.39 \pm 0.16$	$16.94 \pm 0.57 \pm 0.24$
201.75	$1.52 \pm 0.32 \pm 0.07$	$7.36 \pm 0.54 \pm 0.12$	$7.98 \pm 0.57 \pm 0.15$	$16.95 \pm 0.85 \pm 0.24$

Table 5: CC03 cross sections for the reactions $\mathrm{e^+e^-} \to \ell\nu\ell\nu(\gamma)$, $\mathrm{e^+e^-} \to qq\ell\nu(\gamma)$ (summed over lepton species), $\mathrm{e^+e^-} \to qqqq(\gamma)$, and the total W-pair cross section, σ_{WW}, as resulting from the fits to the data at the four centre-of-mass energies. The total W-pair cross sections as expected in the Standard Model, calculated with GENTLE [29], are 16.95 pb, 17.25 pb, 17.45 pb, and 17.52 pb respectively at the four centre-of-mass energies. The theoretical error on these predictions amounts to 2% [3, 4]. Recent preliminary predictions of other programs are 2.0% to 2.8% lower [32, 33].

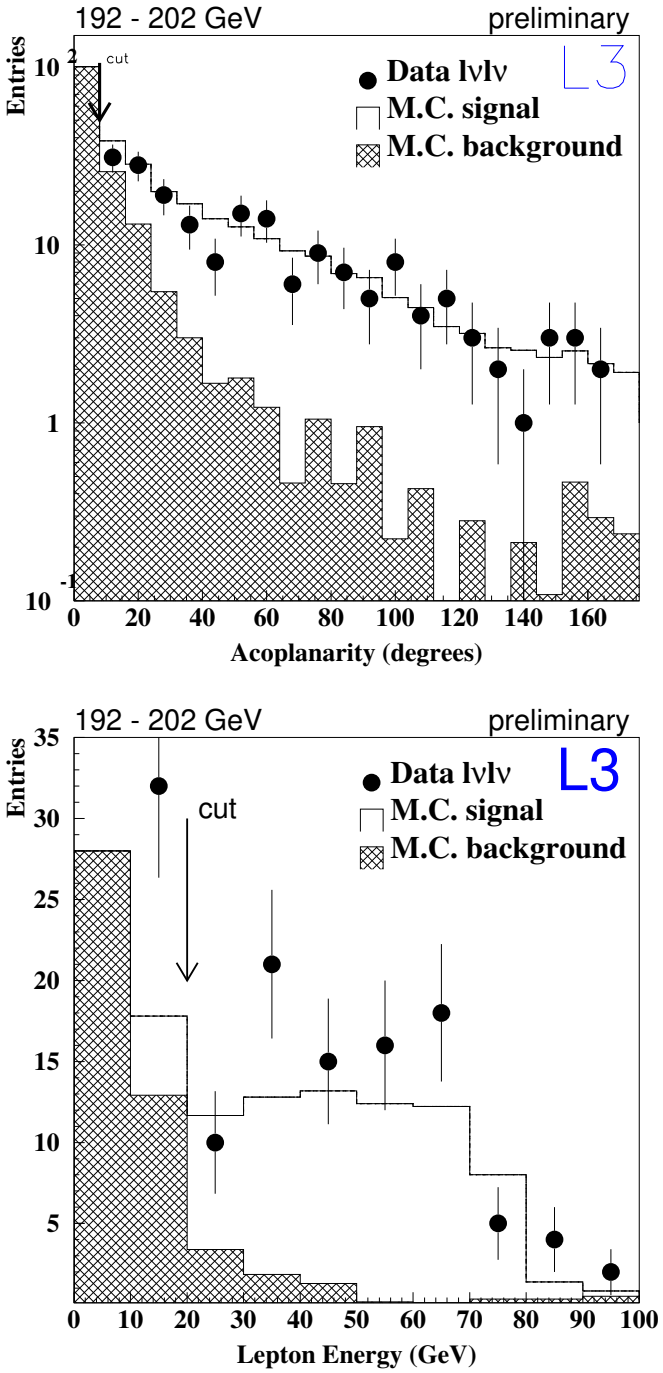

Figure 1: Distributions of variables used for the selection of $e^+e^- \to \ell\nu\ell\nu(\gamma)$ events, comparing the signal and background Monte Carlo to the data. The position of the selection cuts are indicated by vertical arrows, see text. All selection cuts except in the variable plotted are applied. (a) The acoplanarity between the two leptons in the lepton-lepton class. (b) The energy of the identified electron or muon in the lepton-jet class.

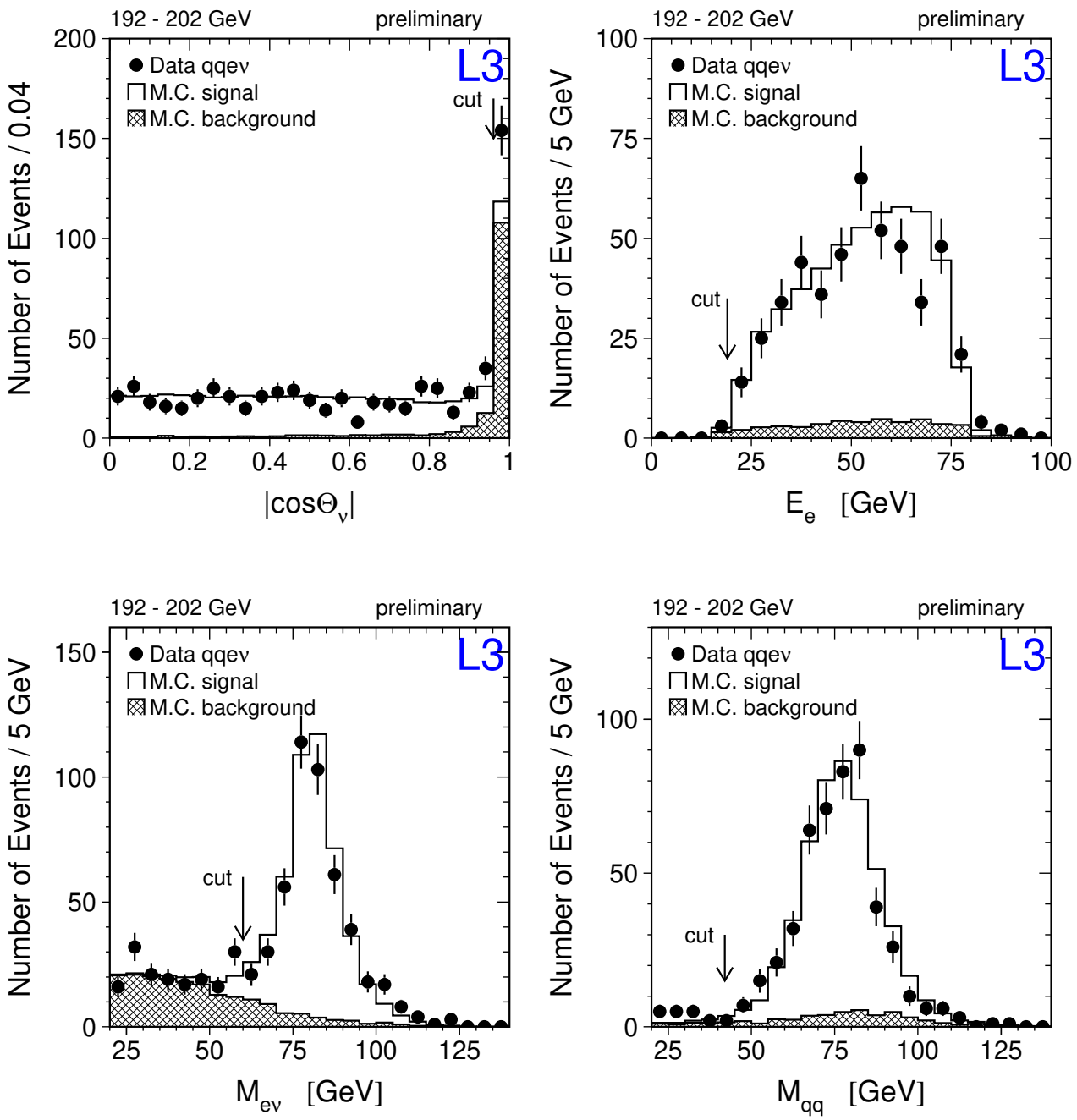

Figure 2: Distributions of variables used for the selection of $e^+e^- \to qqe\nu(\gamma)$ events with the electron identified in the BGO electromagnetic calorimeter. (a) The polar angle of the neutrino, $|\cos\theta_\nu|$. (b) The energy of the electron E_e. (c) The invariant mass of the electron-neutrino system, $M_{e\nu}$. (d) The invariant mass of the jet-jet system, M_{qq}.

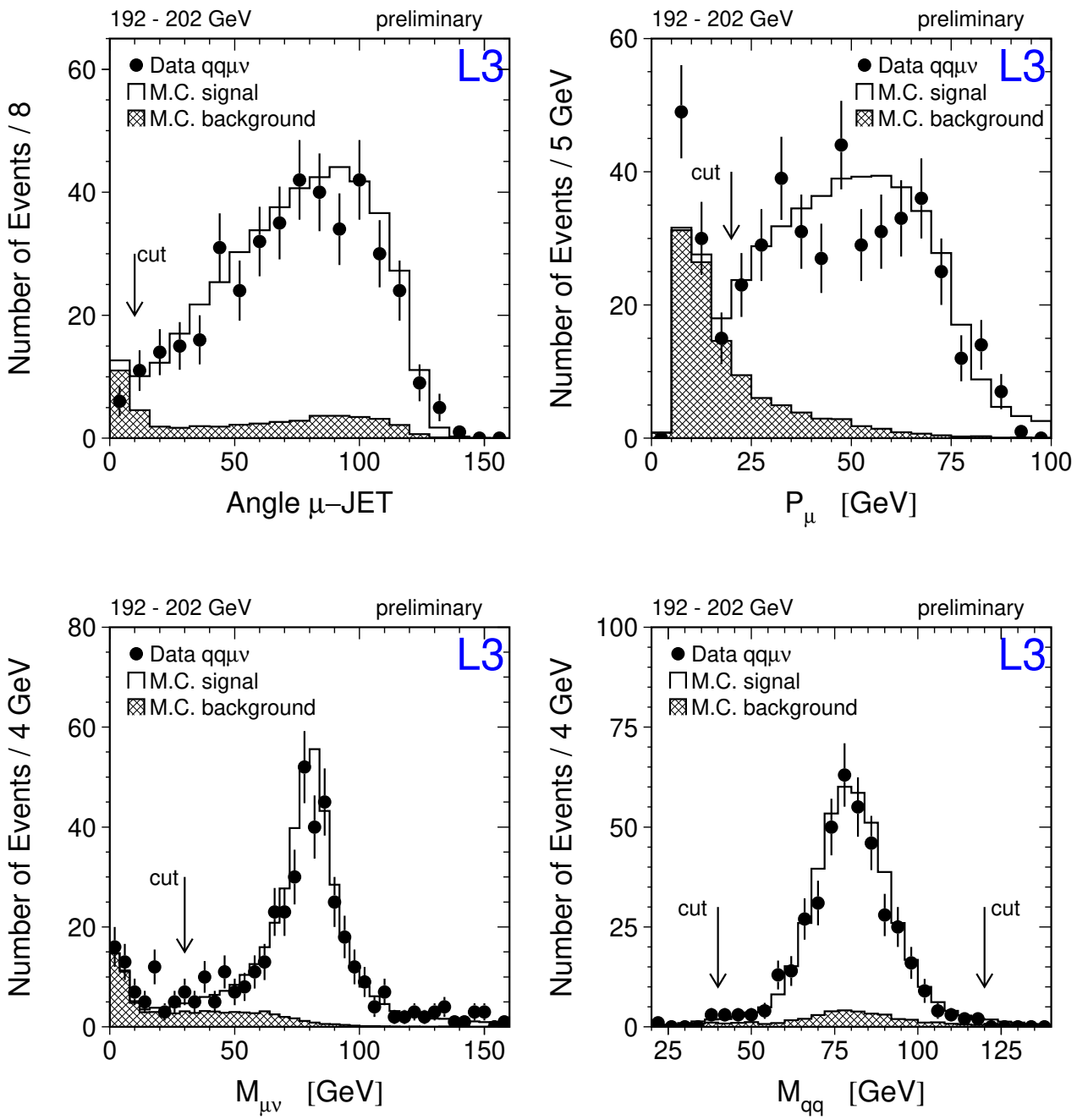

Figure 3: Distributions of variables used for the selection of $e^+e^- \to qq\mu\nu(\gamma)$ events. (a) The angle between the muon and the nearest of the two reconstructed hadronic jets, in degrees. (b) The momentum of the muon p_μ. (c) The invariant mass of the muon-neutrino system, $M_{\mu\nu}$. (d) The invariant mass of the jet-jet system, M_{qq}.

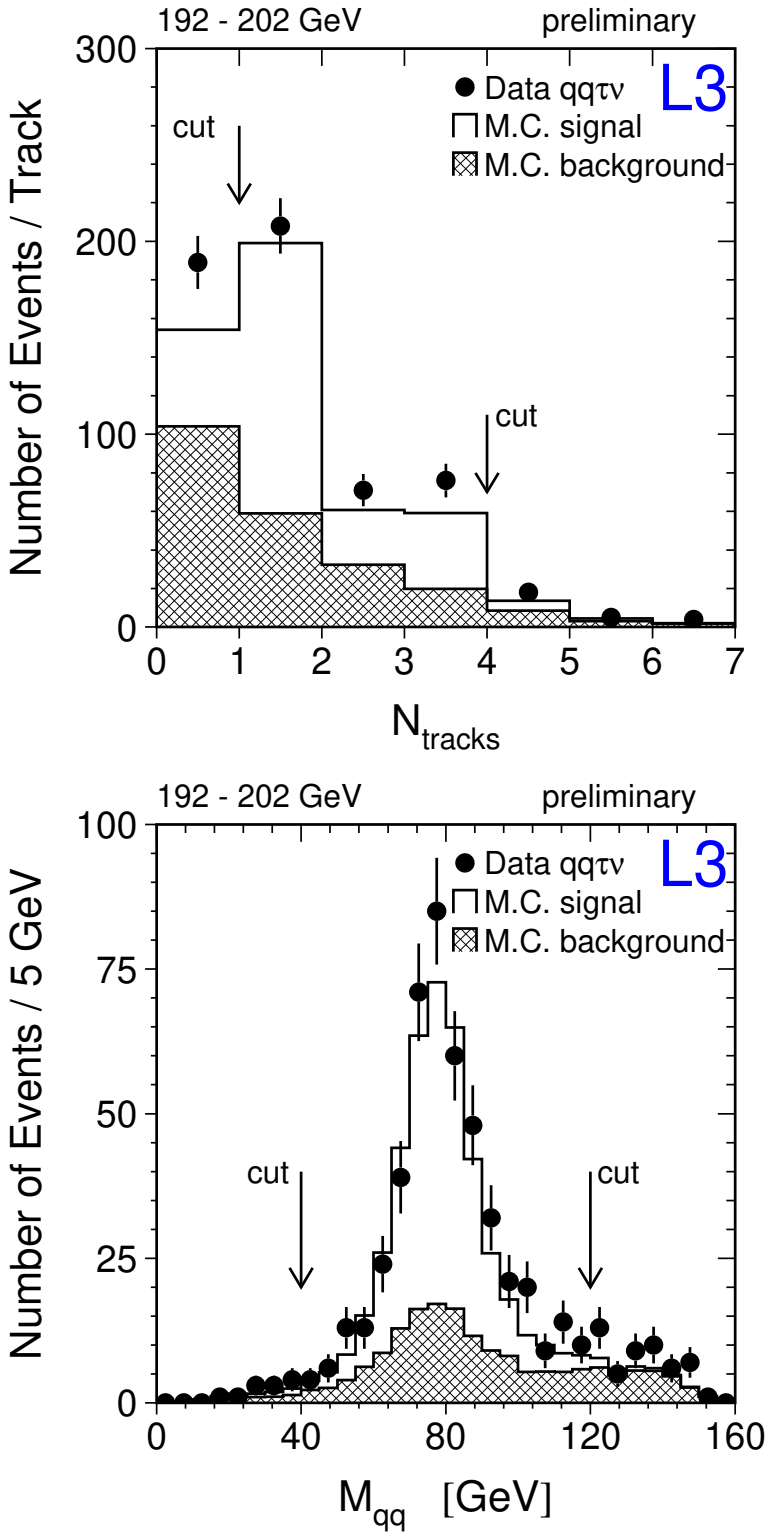

Figure 4: Distributions of variables used for the selection of $e^+e^- \to qq\tau\nu(\gamma)$ events. (a) The number of TEC tracks associated to the τ jet, N_{tracks}. (b) The invariant mass of the jet-jet system, M_{qq}.

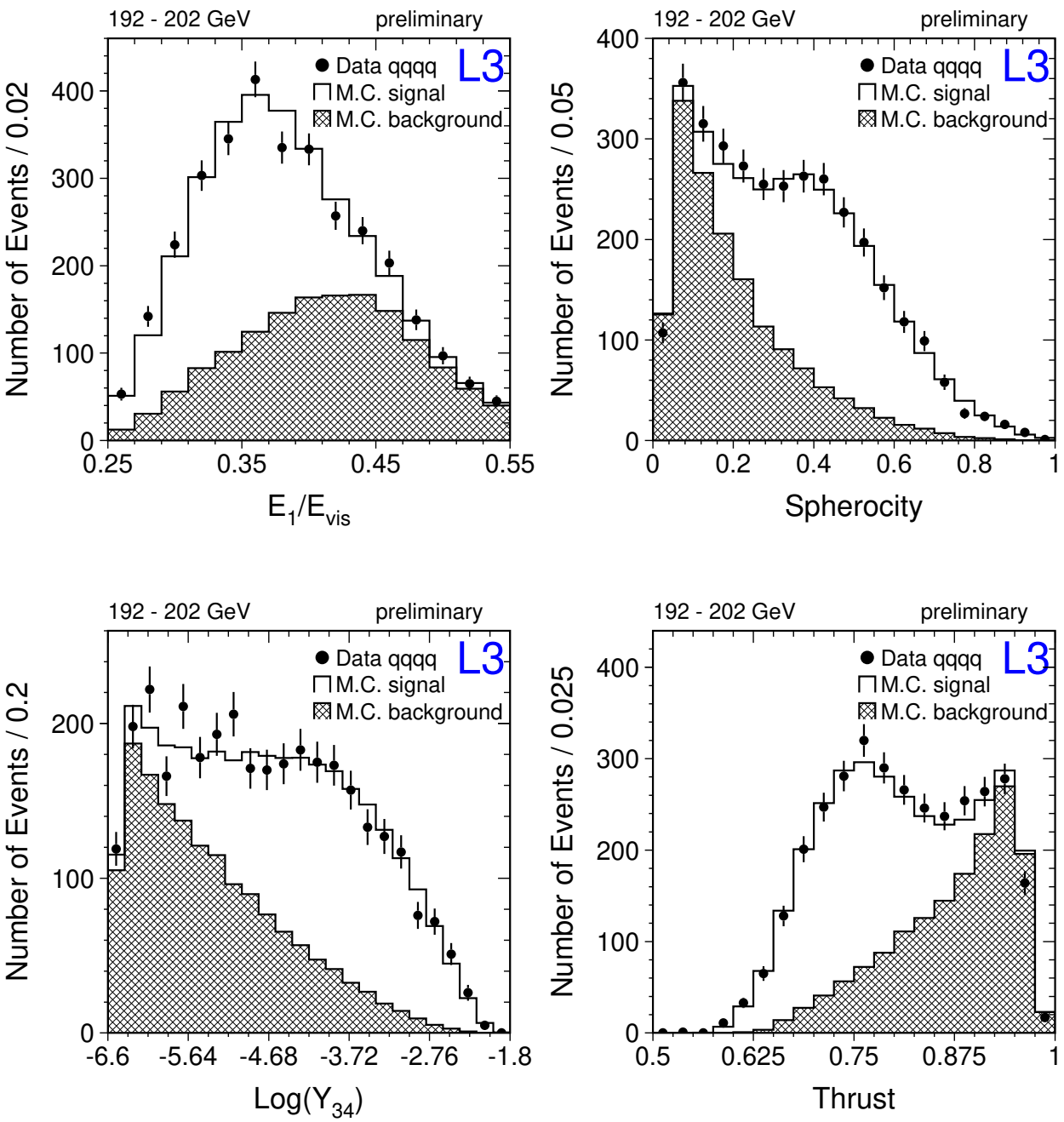

Figure 5: Distributions of variables used for the neural network in the analysis of $e^+e^- \to qqqq(\gamma)$ events or describing the event shape of the hadronic final state. All selection cuts are applied. (a) The scaled maximal jet energy, $E_1/E_{\rm vis}$. (b) The spherocity. (c) $\log y_{34}$. (d) The thrust.

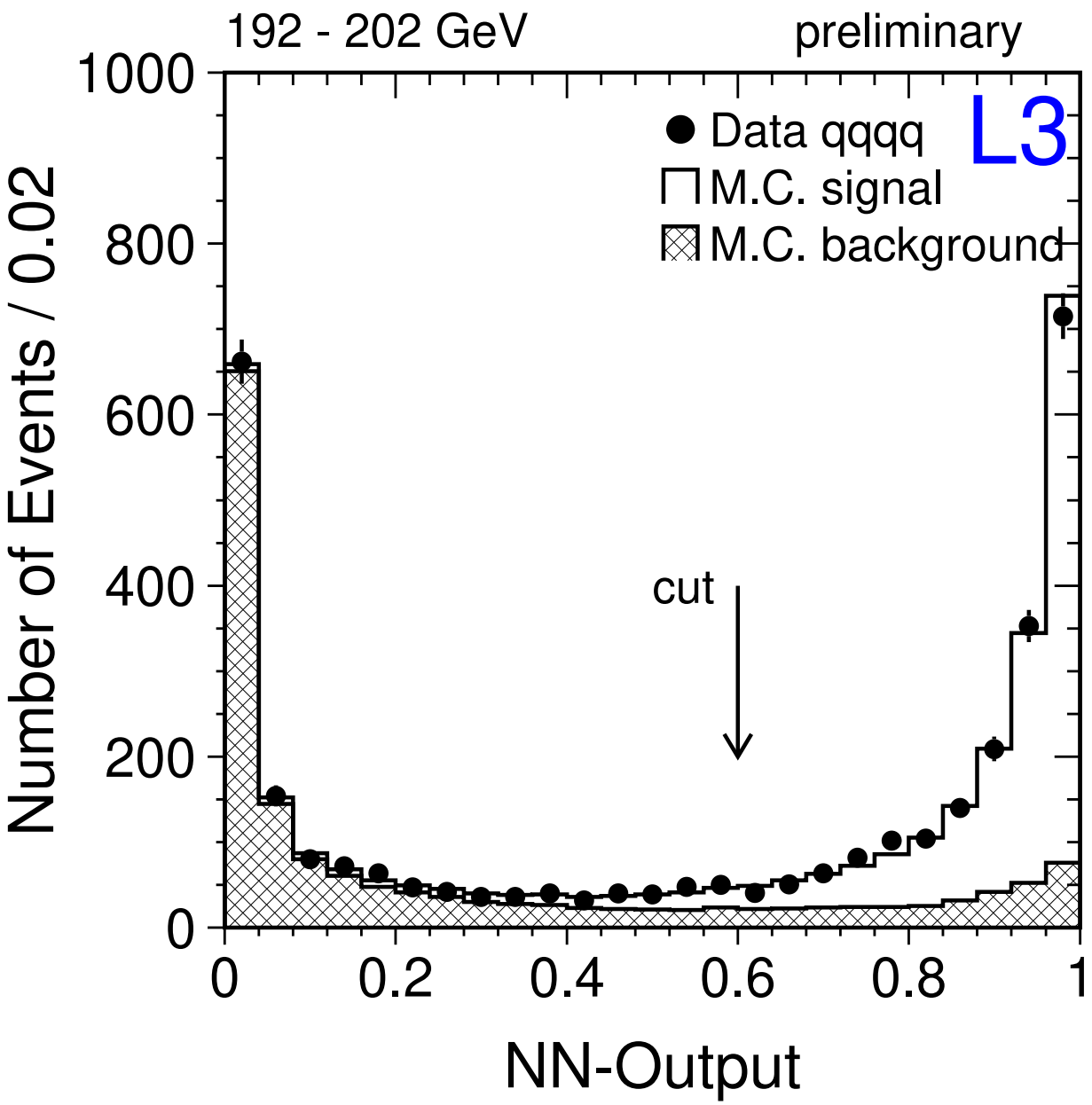

Figure 6: Distribution of the output of the neural network used in the analysis of $e^+e^- \to qqqq(\gamma)$ events.

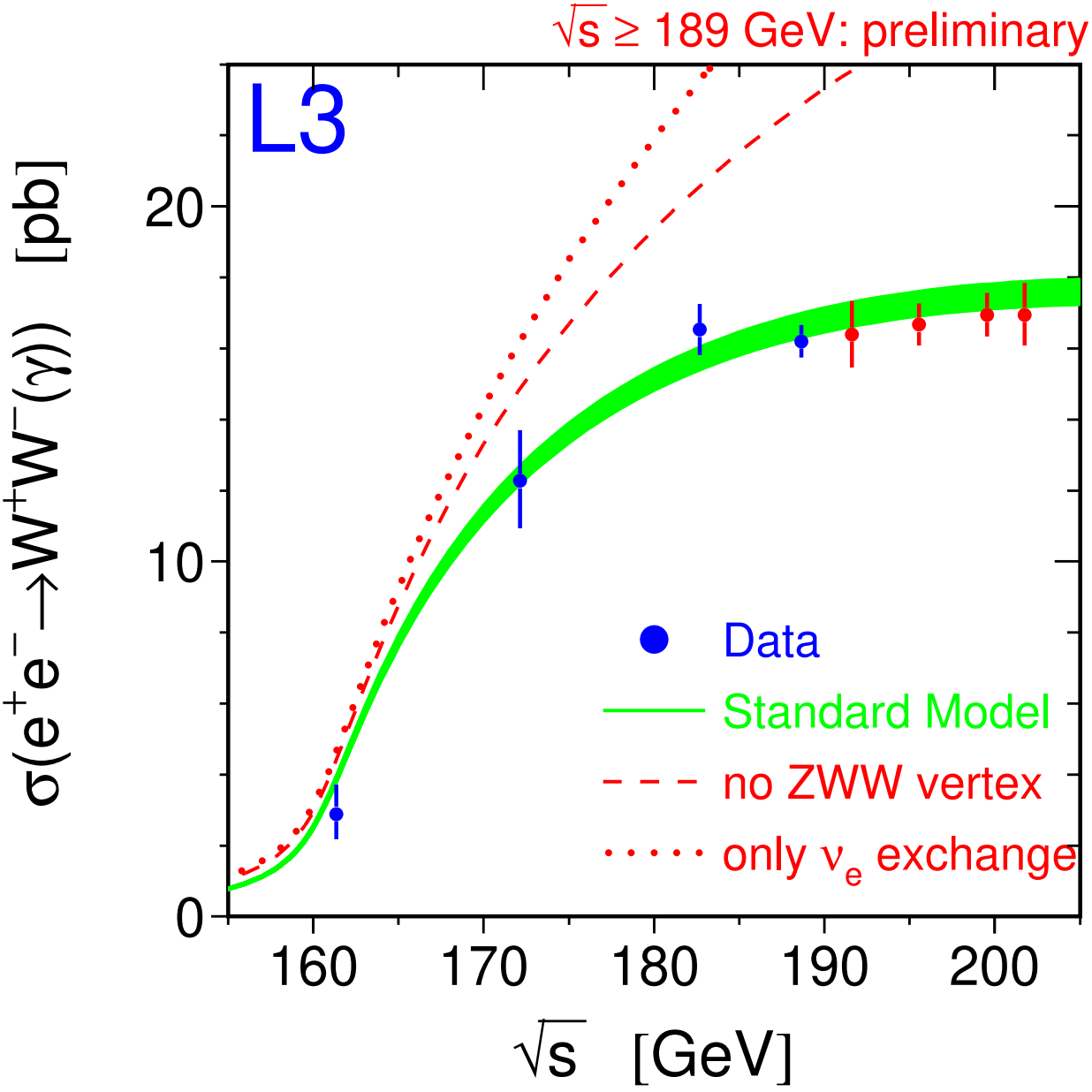

Figure 7: The cross section, σ_{WW}, of the process $\mathrm{e^+e^-} \to \mathrm{WW} \to ffff(\gamma)$ as a function of the centre-of-mass energy, $\sqrt{s}$. The published measurements of σ_{WW} at $\sqrt{s}$ of 161 GeV, 172 GeV, 183 GeV, the preliminary measurement at $\sqrt{s} = 189$ GeV, and the new preliminary measurements at $\sqrt{s} = 192$ GeV, 196 GeV, 200 GeV and 202 GeV are shown as dots with error bars, combining statistical and systematic errors in quadrature. The solid curve shows the Standard Model expectation as calculated with GENTLE [29]. The dashed curve shows the expectation if there is no ZWW coupling. The dotted curve shows the expectation if only t-channel ν_{e} exchange in W-pair production is considered. The theoretical error on the GENTLE cross section amounts to 2% [3, 4] and is indicated as the shaded band.